Angle-of-Incidence Effects in the Spectral Performance of the Infrared Array Camera of the Spitzer Space Telescope

Manuel A. Quijada[a], Catherine Trout Marx[b], Richard G. Arendt[c] and S. Harvey Moseley[b]

[a]Swales Aerospace, 5050 Powder Mill Road, Beltsville, MD 20705
[b]NASA Goddard Space Flight Center, Greenbelt, MD 20771
[c]SSAI, Lanham, MD 20706

ABSTRACT

The Infrared Array Camera (IRAC) on board the Spitzer Space Telescope uses two dichroic beamsplitters, four interference filters, and four detector arrays to acquire images in four different channels with nominal wavelengths of 3.6, 4.5, 5.8, and 8 μm for channels 1 through 4 respectively. A ray-tracing analysis of the IRAC optical system indicates a distribution of angles that is position-dependent at each optical element and the focal-plane arrays. For the band-pass filters in channels 1 and 2, the angle distribution relative to the filter surface normal is 0-28°, whereas for channels 3 and 4, the distribution is from 30° to 58°. Since these angle variations will cause changes in the center-band wavelengths for these interference filters that needed to be accounted for, we performed spectral performance measurements as a function of the angle of incidence on witness samples corresponding to each of the four filters and the two beamsplitters in the IRAC instrument. These measurements were done in the 2-10 μm wavelength range and at the temperature of 5 K, which is near the operating temperature of IRAC. Based on these filter measurements, we also performed an analysis of the pass-band wavelength distributions as a function of position on the instrument focal-plane array detectors. This information is necessary to attain the highest possible photometric accuracy when using IRAC for astronomical observations.

Keywords: Cryogenic, infrared, space flight optics, transmittance, interference band-pass filters

1. INTRODUCTION

The Spitzer Space Telescope, formerly known as the Space Infrared Telescope Facility (SIRTF) contains three focal plane instruments, one of which is the Infrared Array Camera (IRAC).[1] With a wavelength coverage spanning 3 to 10 μm, high-sensitivity detectors, high spatial resolution, and large field-of-view the IRAC instrument will provide astronomers with an unprecedented set of tools for exploring exciting new astrophysical terrain and for addressing many key questions in astronomy today. The IRAC instrument will address the four major scientific objectives defining the Spitzer Space Telescope mission. These objectives are (1) to study the early universe, (2) to search for and study brown dwarfs and superplanets, (3) to study ultraluminous galaxies and active galactic nuclei, and (4) to discover and study protoplanetary and planetary debris disks. In addition, IRAC is a general-purpose camera that will be used by observers on Spitzer Space Telescope for a wide variety of astronomical research programs.

2. IRAC OPTICAL SYSTEM

IRAC is a four channel camera that provides simultaneous images at 3.6, 4.5, 5.8, and 8 μm. The two short wavelength channels use InSb detectors and the two longer wavelength channels use Si:As IBC detectors. Each detector array has 256×256 pixels with a pixel field of view of 1.2 arcseconds, so that each image covers a 5.12×5.12 arcmin total field of view. The optical layout for the IRAC instrument is shown in Fig. 1. This figure also shows the coordinate system of the Spitzer telescope. IRAC views simultaneously two nearly adjacent fields of view near the center of the Spitzer Space Telescope focal plane. A pickoff mirror reflects the light into the camera housing. Each of these fields is split into two channels by the dichroic beamsplitter, with the 3.6 and 5.8 μm channels in one field of view and the 4.5 and 8.0 μm channels in the other. Each field of view has a

Send correspondence to M.A.Q.: E-mail: mquijada@swales.com

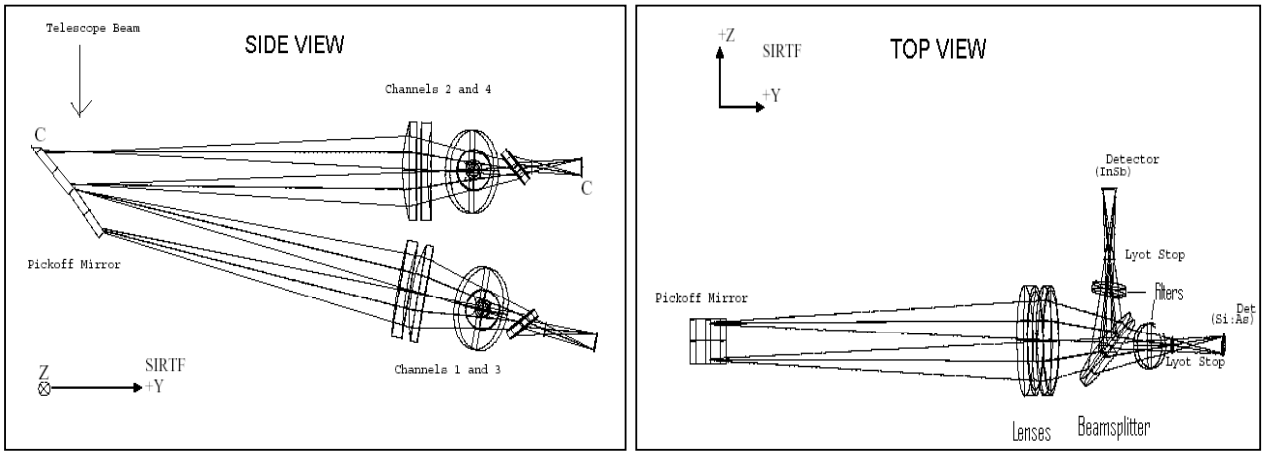

Figure 1. Layout of the IRAC instrument.

lens doublet that reimages the Spitzer Space Telescope focal plane (located near the pickoff mirror) onto the detector arrays. For Channels 1 and 3 the lens materials are MgF2 and ZnS. For Channels 2 and 4 the lenses are ZnSe and BaF2. The beamsplitters reflect the short wavelength and transmit the long wavelength bands, and a Lyot stop is placed at the pupil to eliminate stray light. The fixed filter in front of each detector defines the bandpass. The beamsplitters and filters were manufactured on high-purity Ge substrates. This material was used because the 0.67-eV bandgap of Ge provides a natural short wavelength blocking below 1.8 m.[4] Because the beamsplitters and filters are in a converging beam, not at a pupil, the angle of incidence of the light ray varies as a function of pupil position and fiel angle. This changes the central band-pass as a function of field angle.

The spectral performance of the beamsplitters and filters of IRAC have been reported elsewere.[3] Table 1 summarizes the basic optical performance parameters for these beamsplitter, whereas Table 2 shows the results for each of the four filters.

Table 1. Beamsplitter performance parameters.

	Beamsplitter 1	Beamsplitter 2
Reflectance (%) (front surface)	90 3.2−4.0μm	95 4.0−5.06 μm
Transmittance (%)	90 5.06−6.50μm	90 6.50−9.50μm
Mean angle of incidence	45°	45°
Diameter (mm)	39.0	39.0
Thickness (mm)	3.9	3.9

3. ANGLE DISTRIBUTION AT FILTERS AND BEAMSPLITTERS

The image quality in the optical design of the IRAC instrument alone meets the wavefront error goal of < 0.05 waves rms over each field of view at all wavelengths in the band-passes in all channels. The filter band-passes were chosen to carry out the mission science objectives described above, as well as to provide maximum sensitivity in each band. For example, comparing the flux detected in the 3.6 and 4.5 μm bands will be a good discriminator in searches for brown dwarfs, and the 5.8 and 8.0 μm bands were optimized to achieve the highest sensitivity for deep galaxy surveys.[2] However, for IRAC to carry out its science goals it is imperative to know precisely the band-passes of all installed filters and beamsplitters. So given the fact that optical transmission of these optical

Table 2. Filter performance parameters for all four channels of IRAC.

	Channel 1	Channel 2	Channel 3	Channel 4
Nominal Wavelength(μm)	3.6	4.5	5.8	8.0
Spectral Bandwidth(%)	20.4	23.3	24.9	37.5
Half-power points(μm)	3.2−4.00	4.00−5.06	5.06−6.50	6.50−9.50
Mean In-Band Transmittance (%)	82	80	66	69
Mean Angle of Incidence	11°	11°	45°	45°
Diameter (mm)	19	19	19	19
Thickness (mm)	3	3	3.9	3.9

components will have variations with the the angle of incidence, a model was constructed to determine the full range of angles of incidence at each optical element, as a function of image position at the focal plane array. At each of 25 field angles, a uniform grid of 132 rays across the telescope entrance pupil were traced through the telescope and the IRAC instrument using the Code V ray-tracing program. The angle of incidence of the rays were recorded at the beamsplitters and filters as a function of field position. These incidence angles calculated for the filters are depicted in Fig. 2. The shades of the fans in this figure correspond to the shades of the total response curves in Fig. 9. The field angles were selected to fill the entire detector in a 5×5 grid for each of the four IRAC channels. The general trend is such that the mean angle of incidence increases with increasing distance from the +Z axis coordinate system of the telescope (see Fig. 2). The fan arrays shown in Fig. 2 indicate the filter angles of incidence that are relevant at each of 25 positions spanning each array. The SIRTF Y-Z coordinate system and boundaries of each array are indicated. In particular, we found that for channels 1 and 2 the angle distribution included the 0−28° range, whereas for channels 3 and 4 the range is 30−58°.

4. TRANSMISSION AND REFLECTION AS FUNCTION OF ANGLE

We now present the optical transmission and reflection of the IRAC filters and beamsplitter as a function of the angle of incidence. But first we discussed the experimental method used to obtain these data.

4.1. Experimental Method

A Bruker IFS113V Fourier transform infrared (FTIR) spectrometer was used for the reflectance and transmittance measurements of these IRAC components. This instrument is a Genzel interferometer with a maximum resolution of 0.03 cm^{-1}. A Ge/KBr beamsplitter was used to cover the operating wavelength of the IRAC instrument of 2 to 25 μm. The data were obtained at a resolution of 4 cm^{-1} using a glow-bar source and a DTGS detector. Transmittance measurements were done at the angle of incidence in the range of 0−30° for channel 1 and 2 filters, and between 30−60° for channel 3 and 4 filters and beamsplitters. To have a better defined angle of incidence in the transmission measurements, the IR beam incident on the sample was set in collimated space with a diameter of 1 inch. The reflectance measurements were referenced to an evaporated Au mirror and the results were corrected for the Au reflectance.

Even though most astronomical sources are expected to show very little polarization, we characterized the IRAC optical components by using polarizers to separate the s and p components of the incident radiation. The polarizers used are commercially available from Cambridge Physical Sciences, Ltd, and they consisted of 0.4 μm Al grids deposited on KRS-5 (ThBrI) substrates. With two of them in the beam, the transmittance of the unwanted polarization component was less than 0.8% between 2 μm and 30 μm.

Samples were tested near the IRAC operating temperature by having them mounted in an Oxford Instruments Optistat CF continuous flow liquid helium cryostat. The cryostat was equipped with ZnSe windows and it was mounted on the vacuum box of the FTIR spectrometer with the optical tail extending into the sample chamber.

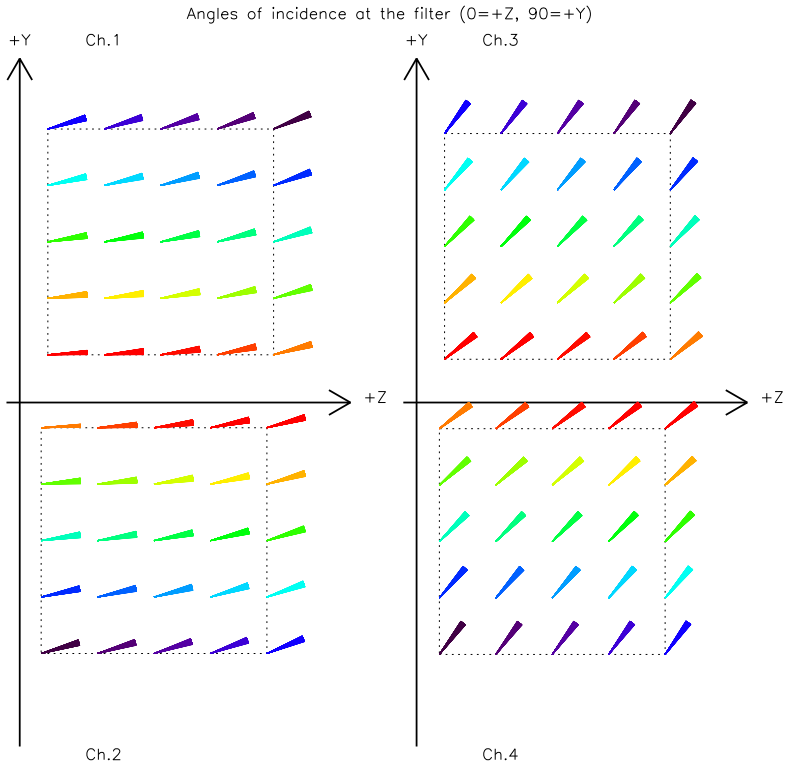

Figure 2. Angle of incidence *at the filters*, for rays arriving at selected locations across IRAC focal plane arrays. A 0° angle of incidence is represented by a horizontal line; a 90° angle would be a vertical line. The width of each "fan" represents the range in angles at each location.

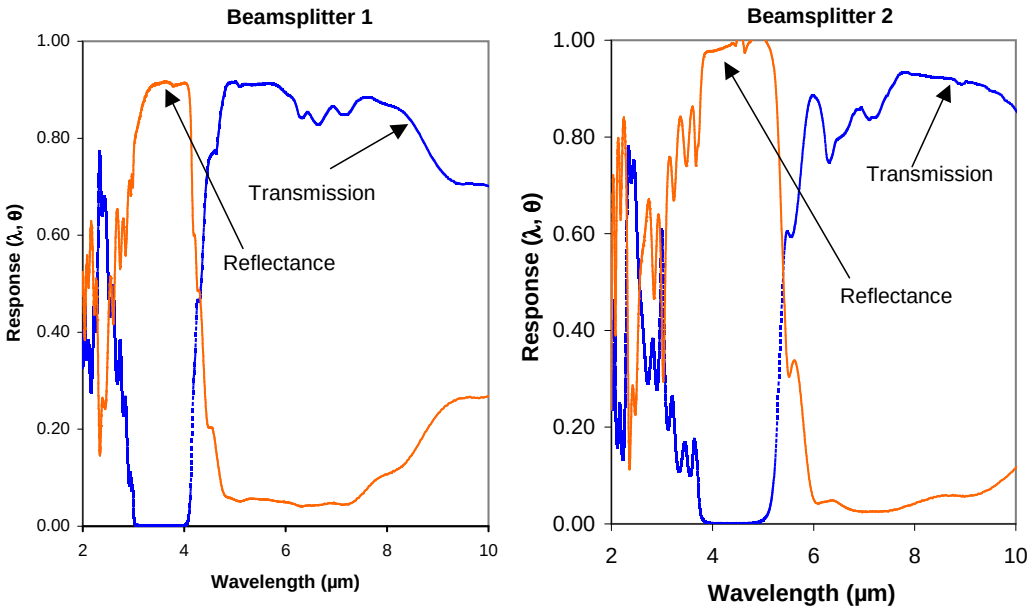

Figure 3. Beamsplitters transmission and reflection for IRAC channels 1 and 3 (left panel); and channels 2 and 4 (right panel) as a function of wavelength at the nominal 45° angle of incidence.

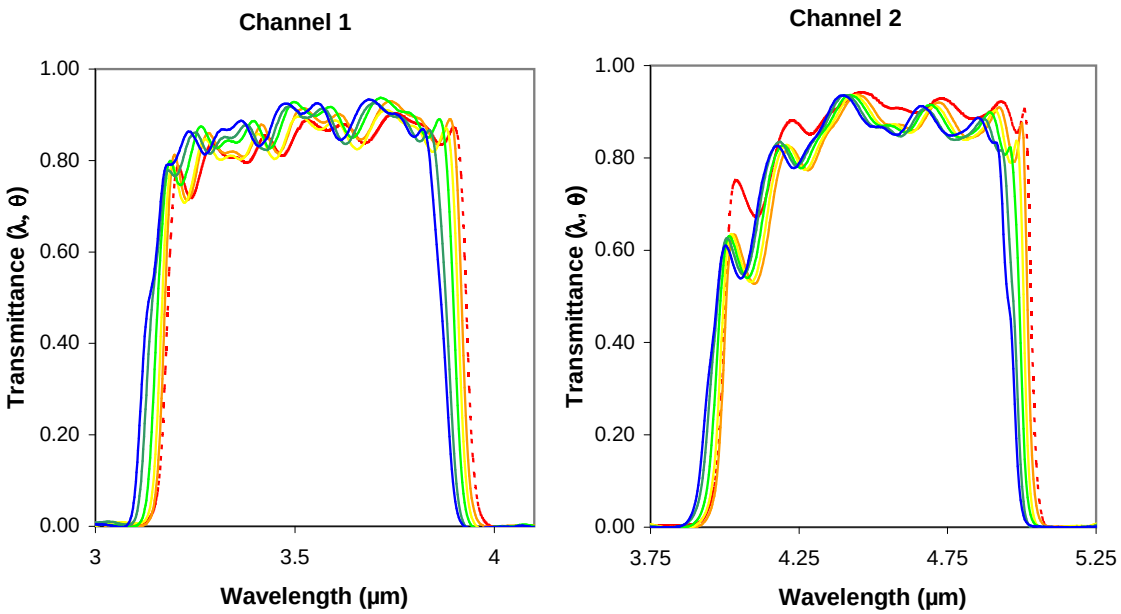

Figure 4. Channels 1 and 2 filter transmission as a function of wavelength at several angles of incidence. As the angle of incidence increases from $\theta = 0°$ through 10°, 15°, 20°, 25°, and 28° the passband shifts towards shorter (bluer) wavelengths.

4.2. Optical Data

The IRAC optical system has two beamsplitters (manufactured by Barr Associates) that operate as low-pass filters at an angle of incidence of 45°, reflecting the incident beam to the short wavelength filter (Channel 1 or 2), and transmitting the incident beam to the long wavelength filter (Channel 3 or 4). The reflectance and transmittance of both beamsplitters are shown in Fig. 3. Beamsplitter 1, shown on the left separates Channels 1 and 3, while beamsplitter 2 on the right separates Channels 2 and 4. Beamsplitter 2 is very similar to number 1, but its low-pass edge occurs 1 μm longer in wavelength, at approximately 5.5 μm.

The four bandpass filters were manufactured by Optical Coating Laboratories, Inc. Figure 4 displays the filter transmission data at 5 K for channels 1 and 2. Each panel shows the transmission progression when the angle of incidence is changed following the sequence 0°, 5°,10°, 15°, 20°, 25°, and 28°. The bandpass for these filters show a uniform shift from long to short wavelengths when the angle of incidence is changed from normal incidence (0°) to the maximum angle of 28°. As we discussed in Sect. 3 this is the range of angles that are of interest for these channels. The angle dependence in the band-pass wavelengths is better illustrated in Fig. 5, where we see a shift towards shorter wavelengths as the angle is changed from normal to the plane of the filters to more oblique angles. This follows from the fact that for interference coatings, there is a reduction in phase difference that occurs at oblique angles between transmitted and reflected waves at the filter interfaces. A simple geometrical analysis[5] yields the angular dependence of the shifted wavelength λ from the equation:

$$\lambda = \lambda_0 \sqrt{1 - \sin^2(\theta)/n^2} \tag{1}$$

where λ_0 is the unshifted wavelength at normal incidence, θ is the angle of incidence and n is the effective refractive index inside the filter.

We now show in Fig. 6 the filter transmission data for channels 3 and 4 at the temperature of 5 K. Like the case for channels 1 and 2, these curves show a progression in the passband from long to short wavelengths when the angle is varied from normal incidence (0°) to the maximum angle of 60°. This trend is better seen in Fig. 7 and Fig. 8. These two figures show how the 50% points of the transmission curves change as a function of the angle of incidence. The overall change is on the order of 5%, which is a significant change given that

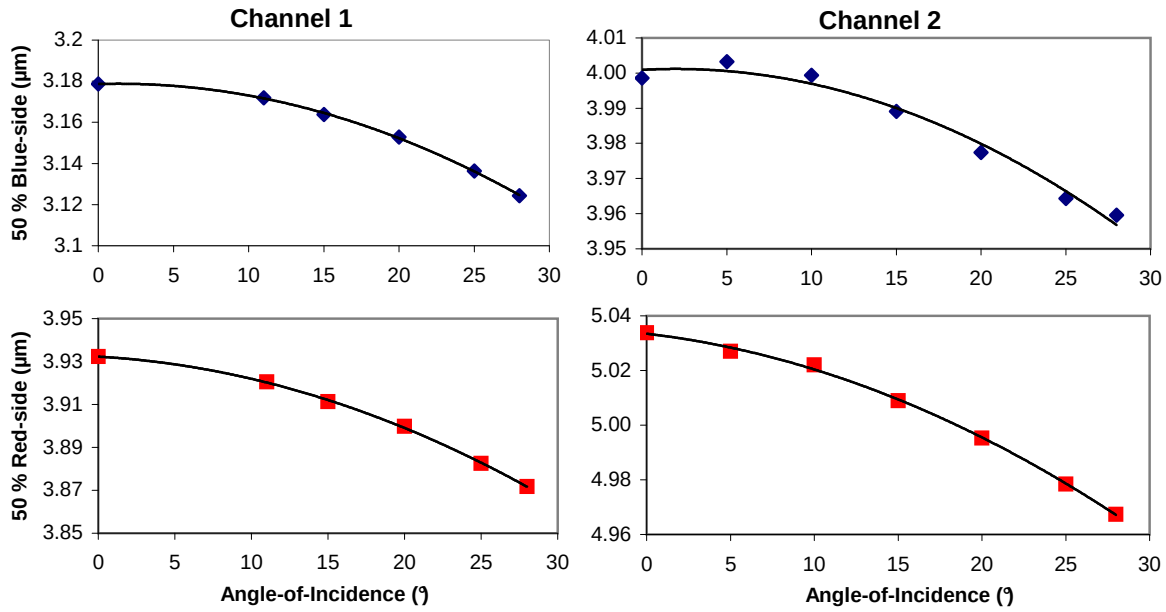

Figure 5. These figures show the 50 % points on the blue- and red-sides for Channel 1 filter (left panels) and channel 2 (right panels) as a function of the angle of incidence. The solid lines are quadratic best-fit results meant to be guide to the eyes. The results for s- and p-polarized light are nearly identical so only the average unpolarized data are shown here.

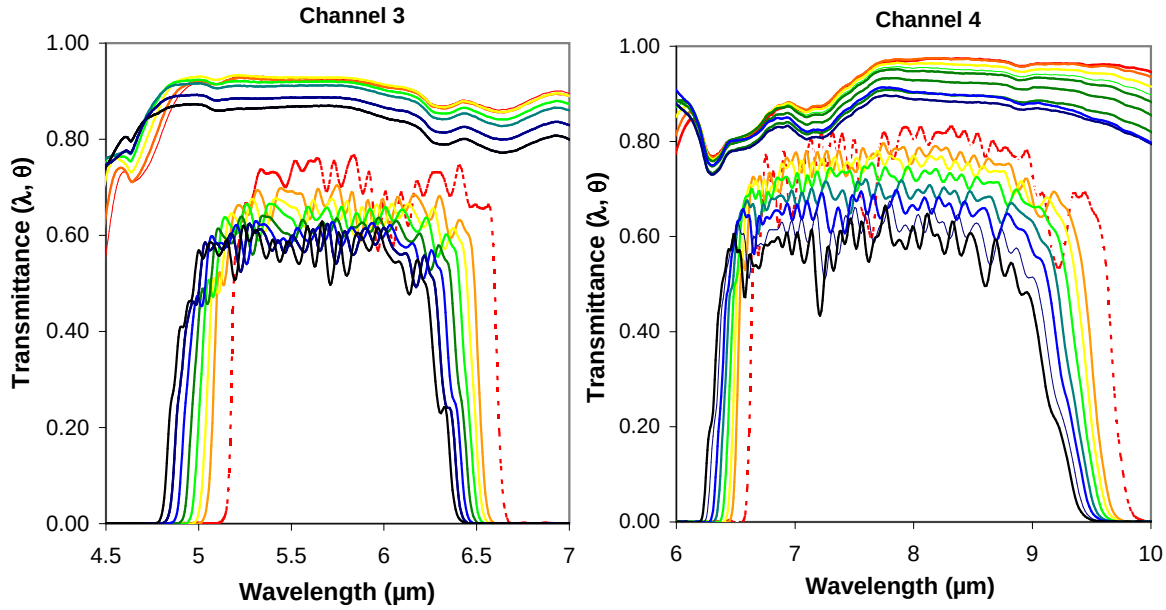

Figure 6. Channels 3 and 4 filter transmission as a function of wavelength at several angles of incidence. The curves show a progression in pass-band from left to right when the angles of incidence are varied in the following sequence: [60°, 55°, 50°, 45°, 40°, 35°, 30°, 0°]. The set of curves above the filter transmission correspond to the transmission for beamsplitters 1 (left) and 2 (right) at the same angles.

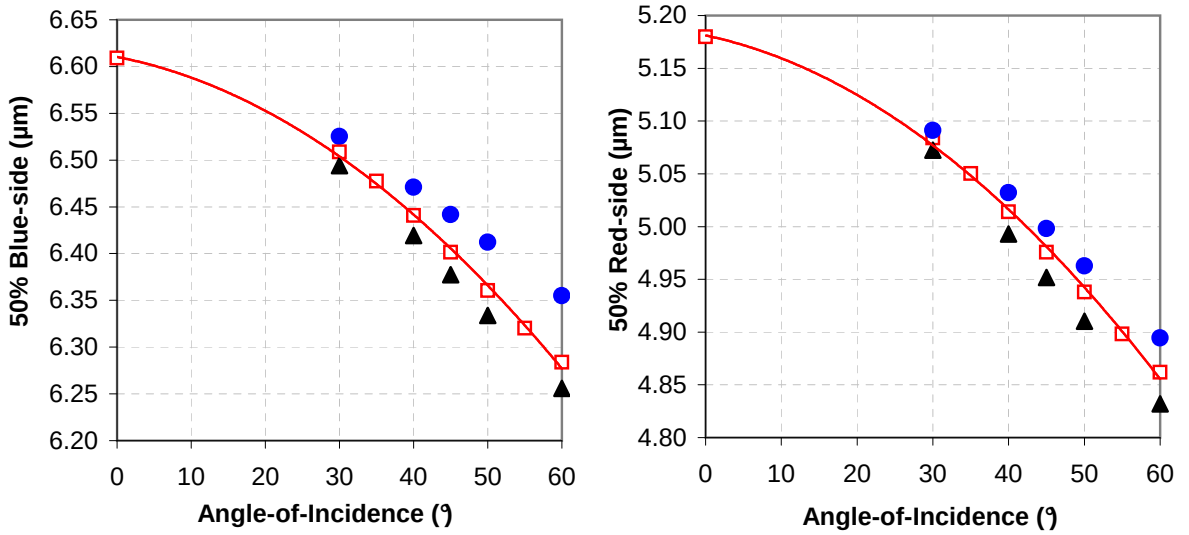

Figure 7. The open squares (along with the best-fit solid lines) represent the unpolarized 50 % points for Channel 3 filter on the blue side (left panel) and red side (right panel) as a function of the angle of incidence. The symbols represent the results for polarized transmission for p-component (circles) and s-component(triangles) for the same filter.

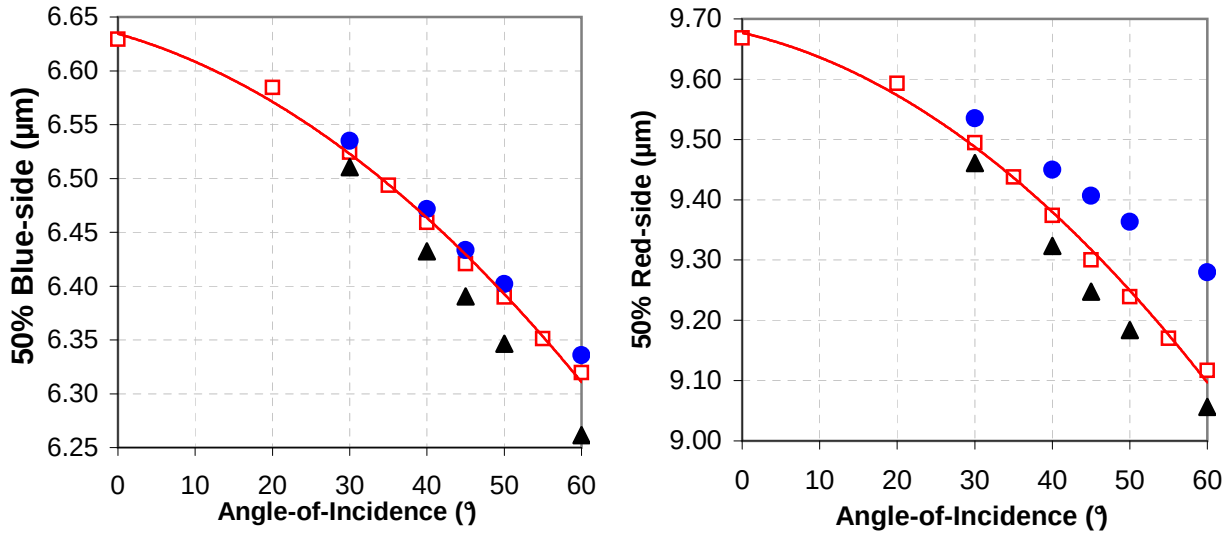

Figure 8. The open squares (along with the best-fit solid lines) represent the unpolarized 50 % points for Channel 4 filter on the blue side (left panel) and red side (right panel) as a function of the angle of incidence. The symbols represent the results for polarized transmission for p-component (circles) and s-component(triangles) for the same filter.

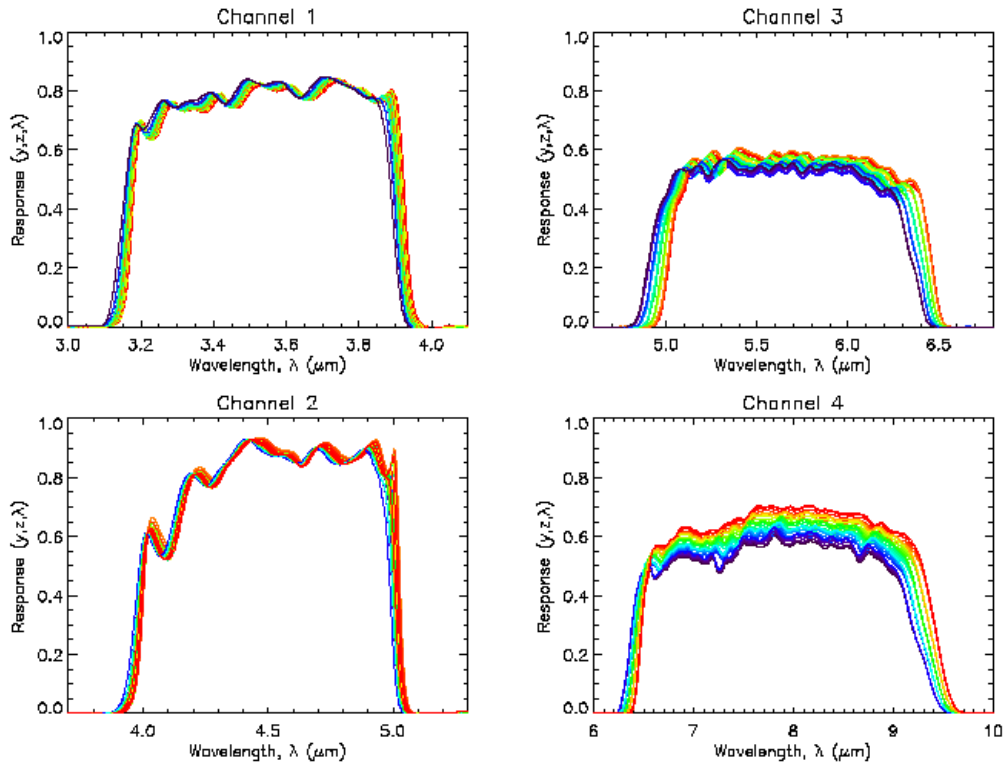

Figure 9. Beamsplitter and filter responses as viewed at the focal-plane array of IRAC. In each panel there are 25 different response curves, color coded to match the focal plane array positions indicated in Fig. 2.

the requirement for the bandpass of these filters to be defined better than 1%. We will discuss in the following section how these data are reduced to simulate the effect this angular dependence will have on the focal plane array of the IRAC optical

5. BANDPASSES AS A FUNCTION OF POSITION

We turn our attention to combining the filter spectral responses with the angle distribution modeled at the IRAC focal plane array shown in Fig. 2. This is done via the equation:

$$R_{yz}(\lambda) = \frac{\int_\theta F_{yz}(\theta)\, T(\lambda,\theta) d\theta}{\int_\theta F_{yz}(\theta) d\theta}, \tag{2}$$

where $R_{yz}(\lambda)$ is the weighted average spectral response at position (y,z) on the focal plane array, $T(\lambda,\theta)$ represents the combined filter+beamsplitter response curves of Fig. 4 and Fig. 6, whereas $F_{yz}(\theta)$ is the light-ray angular distribution fuction depicted in Fig. 2. The resulting $R_{yz}(\lambda)$ for each channel is shown in Fig. 9. In channels 1 and 2, the total spectral response gets bluer (shift to shorter wavelength) with increasing distance from the telescope optical axis (X-Z origin). In channels 3 and 4, the spectral response shifts bluer primarily with increasing distance from +Z axis. These responses have not included those of the telescope optics or the individual detector arrays. The different shades used to plot the lines correspond to those used in Fig. 2 to distinguish the 25 locations at which filter and beamsplitter angles of incidence were modeled.

6. ASTRONOMICAL CONSEQUENCES

Because of the shift in bandpasses, an astronomical source observed with IRAC may produce different instrumental fluxes when observed in different parts of the focal plane array. This variation cannot be automatically

calibrated by a standard data pipeline, because it will depend on the spectrum of the observed source. Astronomers using IRAC data will have to account for this variation in their analysis. Most astronomers working with infrared data are familiar with the application of "color correction factors" (K), which are the ratios of the *effective* bandwidths (i.e. the integrated filter responses weighted by the source spectra) of the astronomical source of interest and the nominal IRAC calibration source spectrum. The nominal wavelengths to which IRAC data are calibrated are chosen to minimize the color correction factors ($0.97 < K < 1.03$ for most sources with smooth continuous spectra). However, color correction factors can easily be $K = 2.0$ or larger for sources with strong spectral bands or lines. Thus, when working with IRAC data, to attain the greatest accuracy, astronomers will have to apply color correction factors to their data, not as a single multiplicative factor per channel (K), but as function of position across each focal plane array [$K(y, z)$]. The net filter+beamsplitter responses reported here are necessary information for calculation of these color correction factors. Detailed discussion of color corrections can be found in the IRAC Data Handbook.*

7. CONCLUSIONS

A geometrical ray-tracing analysis of the IRAC instrument showed that light rays making it through the optical system will have a distribution of angles of incidence at the instrument focal plane array. Given that the pass bands of IRAC four channels were defined by multilayer of dielectric coatings, the spectral performance of these filters and beamsplitters show that angle-of-incidence effects must be taken into account when analyzing data taken with IRAC instrument. Using the measurements described here, astronomical observations can be corrected for the position-dependent bandpasses to yield the greatest possible accuracy from IRAC observations. Finally, the analysis performed in this work was only carried out for the unpolarized responses of the filter+beamsplitter combinations. Given the fact that the filters for channels 3 and 4 show substantial polarization in their s- and p-bandpass responses, additional corrections may be necessary when using the IRAC instrument to study strongly polarized astronomical sources.

ACKNOWLEDGMENTS

We would like to acknowledge George Allen (Barr Associates, Inc.) for useful discussion on the basic theory of interference coating design. We would also like to acknowledge Jim Heaney (Swales Aerospace) for useful discussions during the cryogenic tests on these IRAC optics.

REFERENCES

1. G. G. Fazio, J. L. Hora, S. P. Wilner, J. R. Stauffer, M. L. N. Ashby, Z. Wang, E. V. Tollestrup, J. Pipher, W. Forrest, C. McCreight, S. H. Moseley, W. F. Hoffmann, P. Eisenhardt, and E. L. Wright, "Infrared Array Camera (IRAC) for The Space Infrared Telescope Facility (SIRTF)," Albert M. Fowler; Ed., *Proc. SPIE Vol.* **3354**, pp. 1024-1031 (1998).
2. M. D. Bicay, M. W. Werner, and L. L. Simmons, "Space Infrared Telescope Facility (SIRTF) Enters Development", *Proc. SPIE Vol.* **3354**, pp. 653-664 (1998).
3. Kenneth P. Stewart, Manuel A. Quijada, "Cryo-transmittance and -reflectance of filters and beamsplitters for the SIRTF Infrared Array Camera," *Proc. SPIE Int., Soc. Opt. Eng.* **4131**, 218 (2000).
4. Paul Klocek, Editor, "Handbook of Infrared Optical Materials" (*Marcel Dekker, New York*), pp.262 (1991).
5. Philip Baumeister, "Optical Coating Technology" (SPIE Press, Bellingham, Washington USA, 2004).

*http://ssc.spitzer.caltech.edu/irac/dh/